Excitability modulations of somatosensory perception do not depend on feedforward neuronal population spikes

T. Stephani[1¶*], A. Villringer[1, 2, 3], V. V. Nikulin[1*]

[1] Department of Neurology, Max Planck Institute for Human Cognitive and Brain Sciences, Leipzig, Germany
[2] Berlin School of Mind and Brain, Humboldt-Universität zu Berlin, Berlin, Germany
[3] Clinic for Cognitive Neurology, University Hospital Leipzig, Leipzig, Germany
[¶] Now at the Donders Institute for Brain, Cognition and Behaviour, Radboud University, Nijmegen, The Netherlands
[*] corresponding authors: T.S. (tilman.stephani@donders.ru.nl); V.V.N. (nikulin@cbs.mpg.de)

Abstract

Neural states shape perception at earliest cortical processing levels. Previously we showed a relationship between the N20 component of the somatosensory evoked potential (SEP), pre-stimulus alpha oscillations, and the perceived intensity in a somatosensory discrimination paradigm (Stephani et al., 2021, eLife). Here we address the follow-up question whether these excitability dynamics reflect changes in feedforward or feedback signals. Re-examining the previous EEG data, we leveraged high-frequency oscillations (HFO) as a metric for neuronal population spiking activity of the first excitatory feedforward volley in the cortex. Using Bayesian statistics, we found evidence against the involvement of HFO in moment-to-moment variability of perceived stimulus intensity, in contrast to previously observed pre-stimulus alpha and N20 effects. Given that the N20 component presumably reflects backpropagating membrane potentials towards the apical dendrites, we argue that top-down feedback processes (e.g., related to alpha oscillations) may thus rely on modulations at distal sites of involved pyramidal cells rather than on output firing changes at basal compartments.

Introduction

The perception of even basic stimulus features, such as their intensity (or mere occurrence), is variable and depends on instantaneous states of the neural system when sensory input arrives in the brain (McCormick et al., 2020; Arieli et al., 1996; Sadaghiani et al., 2010; Waschke et al., 2021). This is puzzling since it prevents an exact mapping between a given sensory input and the brain´s response. Recent work has argued that this variability both in neural responses and perceptual outcome is related to dynamics of excitability levels, specifically during early sensory processing in the cortex (Samaha et al., 2020). This may form the neurophysiological basis for behavior- and context-dependent adaptability of sensory information uptake in widely different environments.

In line with this, we recently observed an interrelation between pre-stimulus alpha oscillatory activity, initial cortical responses, and the subjectively perceived stimulus intensity in the human somatosensory system (Stephani et al., 2021). In this work, we analyzed the initial cortical response in the electroencephalogram (EEG), the N20 component of the somatosensory evoked potential (SEP), as a marker of cortical excitability since the N20 is known to only reflect excitatory processes of the first thalamo-cortical volley arriving in the primary somatosensory cortex (S1) in Brodmann area 3b (BA 3b; Allison et al., 1991; Wikström et al., 1996; Nicholson Peterson et al., 1995; Bruyns-Haylett et al., 2017). This initial thalamo-cortical excitation has been shown to start in middle layers of S1 (i.e., layer 4), leading to a depolarization of basal dendrites near the soma of pyramidal cells (in layer 2/3 and potentially also in layer 5; Kulics & Cauller, 1986). Due to cortical folding, the resulting N20 dipole is oriented tangentially. Importantly, its positive pole points in anterior direction. Together with the morphology of the involved pyramidal cells in BA 3b (i.e., posterior-to-anterior direction of soma to apical dendrites), this dipole polarity suggests that the N20 potential spreads from the basal compartments of involved pyramidal cells (where sensory inputs arrive) not only to the soma where axonal action potentials are generated but also along the membranes towards the apical dendrite of the pyramidal cell (Fig. 1; Wikström et al., 1996). This notion of a backpropagating membrane depolarization following the N20 has been further supported by invasive recordings in non-human animals (Ikeda et al., 2005), as well as by recent biophysical modeling work (Thorpe et al., 2024). Thus, the N20 most likely spans several compartments of the involved pyramidal cells (i.e., basal dendrites, soma, and apical dendrites) in different cortical layers.

At the same time, different compartments of pyramidal cells have been proposed to serve distinct functional roles (Larkum, 2013): While feedforward input (i.e., sensory information) arrives at basal dendrites near the cell soma, the apical dendrites in superficial layers receive and integrate top-down signals from corticocortical and thalamocortical feedback loops (i.e., contextual information). In a "coupling zone" in the proximal apical dendrite, the combination of these two information streams takes place (Aru et al., 2020). Here, dendritic Ca^{2+} potentials enable a communication between distant but coinciding depolarization events at apical and basal dendritic sites, which crucially also involves the backpropagation of membrane potentials from basal towards apical compartments (Larkum et al., 2004; Larkum et al., 1999). This leads to a modifiable interaction between bottom-up sensory input and top-down contextual information on a cellular level (Phillips et al., 2015; Aru et al., 2020). This may form a neurophysiological basis for the modulatory role of instantaneous brain states on perception, such as related to arousal, prediction, or other cognitive states (Phillips et al., 2016; Larkum, 2022; Marvan et al., 2021; Aru et al., 2020; Bachmann et al., 2020), referred to as *Dendritic Integration Theory*.

Thus, in the context of somatosensory excitability fluctuations that we recently found to be reflected in N20 amplitudes (Stephani et al., 2021), the question arises whether these effects take place via top-down modulatory states in superficial layers or rather relate to changes of feedforward output firing in middle layers.

Non-invasive EEG cannot answer this question of layer-specific activity directly. However, it is possible to study so-called high-frequency oscillations (HFO), which have been shown to correspond to

neuronal population spikes during the initial thalamo-cortical excitatory volley in response to median nerve stimulation (Baker et al., 2003; Curio, 2000; Shimazu et al., 2000). HFO reflect phase-locked activity at frequencies above 500 Hz and at latencies just around the peak of the N20 component (e.g., Waterstraat et al., 2021). They have been associated both with thalamic as well as cortical generators in BA 1 and BA 3b (Gobbelé et al., 2000; Shimazu et al., 2000). While HFO before the peak of the N20 may reflect thalamo-cortical spiking, HFO of purely cortical origin in BA 3b can be identified based on their tangential dipole topography (Gobbelé et al., 2004) and their onset at or just after the N20 peak (Baker et al., 2003; Ritter et al., 2008). It has been shown that the cortical HFO in BA 3b originate from very similar sources as the N20 (Ikeda et al., 2005; Shimazu et al., 2000), engage in initial cortical processing of naturalistic tactile information like the N20 (Baker et al., 2003), but reflect a physiologically different process than the N20 on a cellular level, that is, the interplay of incoming and outgoing action potentials of the involved pyramidal cells (likely in a fast exchange with neighboring interneurons in cortex layer 4; Hu et al., 2023; Ozaki & Hashimoto, 2011). Thus, in the context of our question, HFO allow to test whether the excitability modulations we observed in our previous study (Stephani et al., 2021) are manifested in neuronal population spikes that occur around the basal compartments of S1 pyramidal cells (middle layers) or rather unfold in post-synaptic membrane potentials – as reflected by the N20 potential – that propagate from the soma "back" towards the apical dendrites (superficial layers).

To this end, we re-analyzed the data of our previous study in which participants performed a somatosensory intensity discrimination task, regarding HFO and their relationship with pre-stimulus alpha activity, the N20 component of the SEP, as well as perceived stimulus intensity. Taken together, we found evidence *against* the involvement of HFO in the modulation of perceived stimulus intensity – in contrast to pre-stimulus alpha and N20 amplitudes – suggesting that behaviorally relevant modulations of cortical excitability may take place at apical rather than basal sites of pyramidal cells at this initial processing stage in S1.

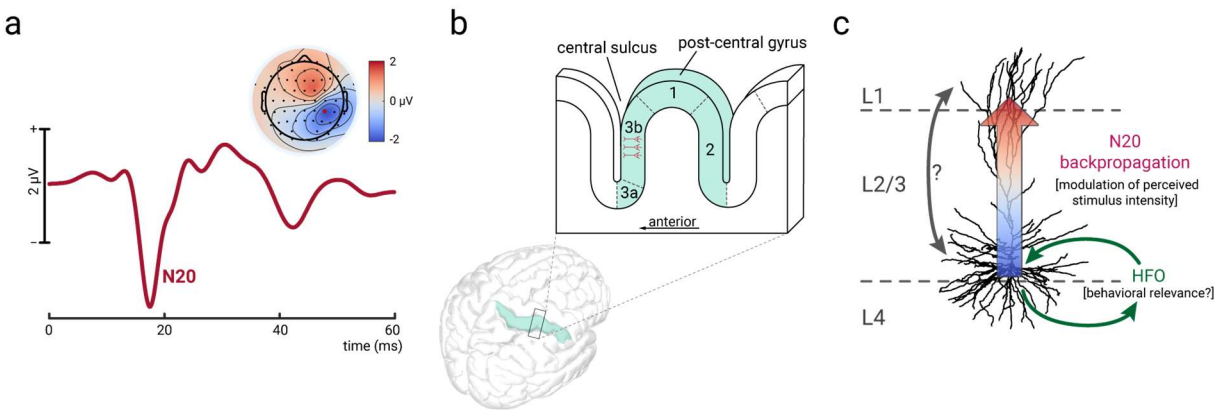

Fig. 1. The N20 component of the somatosensory evoked potential (SEP) and its assumed generation. a) N20 component measured on scalp level with electroencephalography (EEG). SEP at electrode CP4, averaged over 1000 trials (exemplary participant). b) Location of pyramidal cells in Brodmann area 3b in the anterior wall of the post-central gyrus, which are believed to be the sources of the N20 potential. c) The N20 component emerges due to membrane depolarizations that propagate back from the basal compartments towards the apical dendrites. High-frequency oscillations (HFO) emerge in middle layers, representing neuronal population spikes that are most likely involved in feedforward inhibition circuits affecting the basal compartments.

Results

Robust high-frequency oscillations (HFO) around the N20 peak

Participants performed a somatosensory discrimination task, in which they were to distinguish between somatosensory stimuli of two slightly different, supra-threshold intensities (Stephani et al., 2021). Irrespective of the presented and perceived stimulus intensities, clear HFO in response to the median nerve stimuli were observed in 27 out of 32 participants, employing a spatial filtering approach using canonical correlation analysis (CCA; Fig. 2). In all of the 27 participants with overall clear HFO, one CCA component was identified that had a spatial activation pattern suggesting an underlying dipole with tangential orientation – strongly resembling the dipole of the N20 potential (see Stephani et al., 2021) – as well as another CCA component that showed a radial spatial pattern (Fig. 2c). Grand averages of both the tangential and radial CCA components of HFO activity are displayed in Figure 2d. Since our focus here is on HFO that have a cortical origin (Gobbelé et al., 2004) and that are likely generated by the same neuronal populations as the N20 potential (Ikeda et al., 2005), we will continue our analyses with the tangential CCA component in the following sections. Noteworthy, for this tangential CCA component, HFO frequencies were observed to be centered around 700 Hz (Fig. 2b), not 600 Hz as described in previous studies measuring HFO at sensor level above the somatosensory cortex (e.g., Waterstraat et al., 2021).

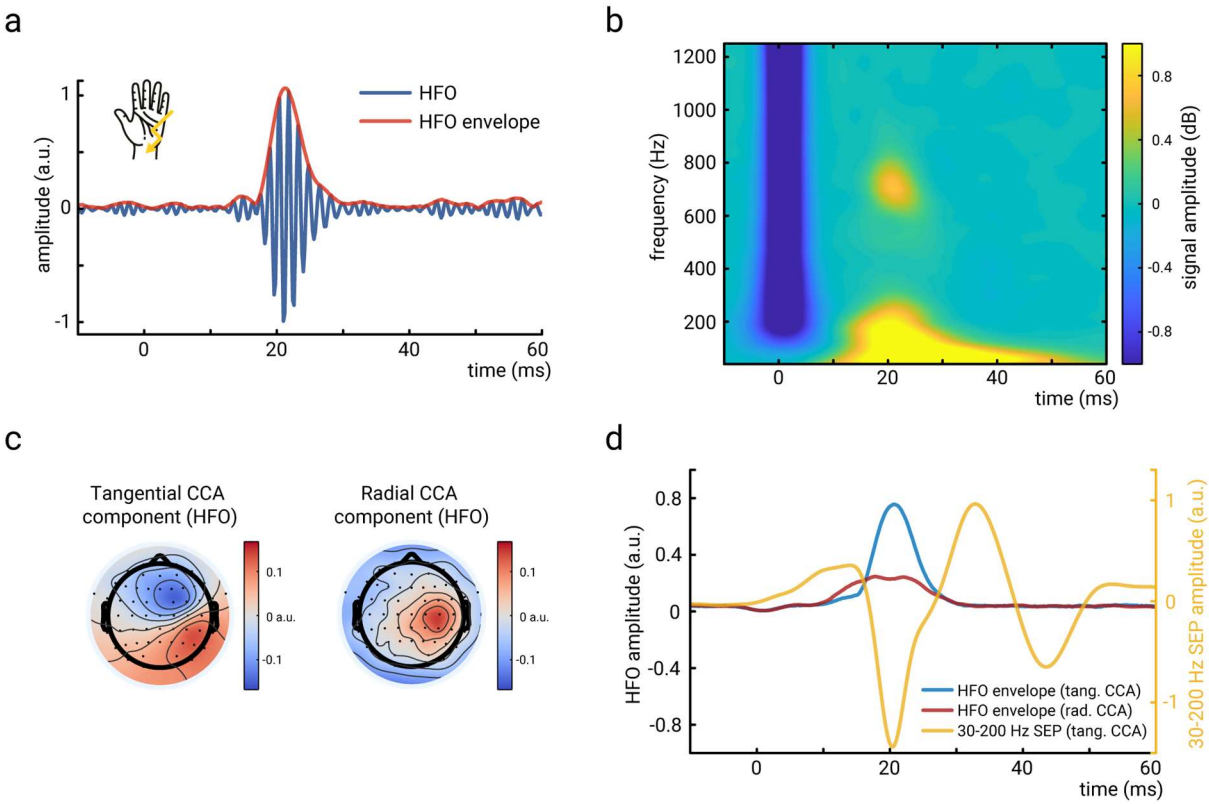

Fig. 2. High-frequency oscillations (HFO) extracted with canonical correlation analysis (CCA). a) HFO of an exemplary participant, averaged over 1000 trials. Displayed are both the stimulus-evoked oscillations as well as their signal envelope (extracted using Hilbert transform). Activity derived from the tangential component of our CCA-based spatial filtering approach. b) Time-frequency representation of the short-latency responses of the somatosensory cortex (averaged across participants; N=27). HFO are visible at 20ms in the frequency range around 700 Hz and are clearly distinct from the conventional SEP in lower frequencies. As in panel a), activity derived from the tangential CCA component. c) Spatial activation patterns of the tangential and radial CCA components computed for HFO (averaged across participants; N=27). d) Grand averages of the HFO envelopes (tangential and radial CCA components) as well as the conventional SEP in the frequency range from 30 to 200 Hz (averaged across participants; N=27). Please note that separate CCAs were performed for HFO and the 30-to-200-Hz SEP (for the latter, see Stephani et al., 2021), both resulting in similar tangential and radial components.

HFO relate to presented but not perceived stimulus intensity

The main objective of this study is to examine whether moment-to-moment fluctuations of the perceived stimulus intensity that we observed in our previous study (Stephani et al., 2021) are also reflected in HFO amplitudes.

To this end, we first tested whether HFO were related even to the minute intensity variations of the presented stimuli in our study (i.e., just above the least-noticeable difference) – which should be expected based on previous literature (Klostermann et al., 1998; Gobbelé et al., 2008) yet with the caveat that these studies compared much bigger intensity differences than us. This comparison is required for the further evaluation of the *perceived* stimulus intensity. Our data confirmed that a higher *presented* stimulus intensity was indeed associated with larger HFO amplitudes (Fig. 3a), as tested both with cluster-based permutation statistics (applied to the within-participant averages, $p < .05$; Fig. 3b), as well as with a linear-mixed-effects model operating on single-trial HFO amplitudes, $\beta = .031$, $t(26349.0) = 2.534$, $p = .011$ (HFO were derived from the tangential CCA component; notably, the size of this intensity effect on HFO was in a similar effect size range as was the case for the N20 component in our previous study, Stephani et al., 2021). As can be seen from Fig. 3b, the presented stimulus intensity modulated HFO amplitudes around their peak (which is congruent with latencies of the N20 peak), with an apparently slightly longer lasting effect after the HFO peak than before their peak.

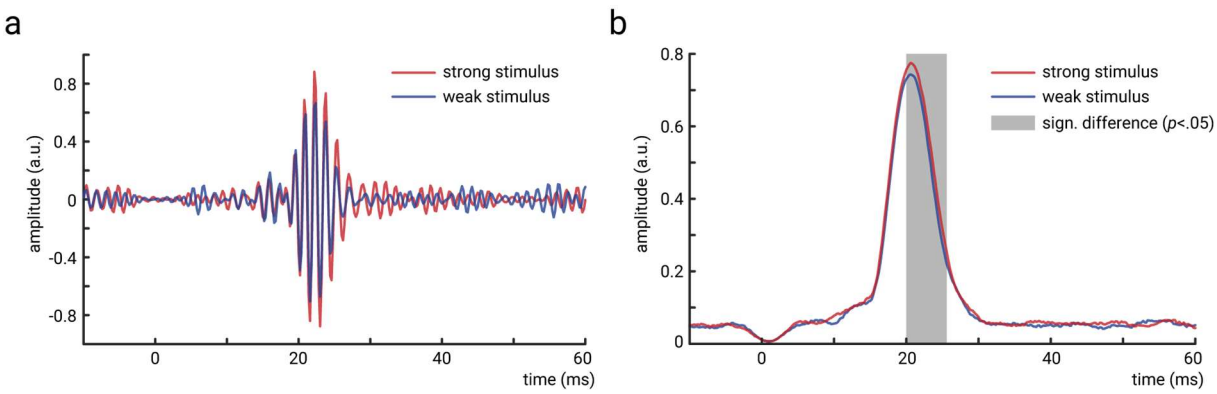

Fig. 3. Effect of presented stimulus intensity on HFO amplitudes. a) Single-participant average of HFO for high and low stimulus intensities. b) Group-level average (N=27) of HFO envelopes for high and low stimulus intensities. Permutation-based cluster statistics indicated a difference shortly after ~20 ms (marked in grey).

Next, we examined the relationship between HFO and perceived stimulus intensity while controlling for the presented stimulus intensity (Fig. 4). For this, we used three approaches: i) adding *HFO amplitude* as additional predictor of *perceived intensity*, next to our previous predictors *pre-stimulus alpha* and *N20 amplitude*, as well as *presented intensity* (Stephani et al., 2021), ii) examining HFO in a separate regression model only including *presented intensity* as a covariate (to account for possible issues of multicollinearity in approach i)), and iii) employing cluster-based permutation statistics separately in the high- and low-intensity conditions.

Adding HFO to our previous regression model did not lead to a better model fit, thus not suggesting any relevance of HFO for perceived stimulus intensity beyond the previously identified predictors, $\chi^2(1) = 0.793$, $p = .373$, $AIC_{incl.\ HFO} = 31170$ vs. $AIC_{excl.\ HFO} = 31169$, $BIC_{incl.\ HFO} = 31219$ vs. $BIC_{excl.\ HFO} = 31210$. Furthermore, HFO effects were not significant in the dedicated regression models only considering HFO and presented stimulus intensity as predictors, $\beta = .012$, $z = 0.860$, $p = .390$. We evaluated these non-significant effects with additional Bayesian statistics, which indicated moderate evidence for the absence of a relationship between HFO and perceived stimulus intensity, BF01 = 4.71, $\beta_{Bayes} = .013$, 95%-credibility interval = [-.014, .040]. Similar evidence was provided by the cluster-

based permutation statistics, which did not show any effect of HFO on perceived stimulus intensity either in the high- or in the low-presented-intensity condition (even with the liberal threshold of a cluster significance level of $p < .1$).

Taken together, spontaneous fluctuations of HFO amplitude thus do not seem to be related to any changes of the *perceived* intensity in our somatosensory discrimination paradigm (when controlling for the physically presented intensity).

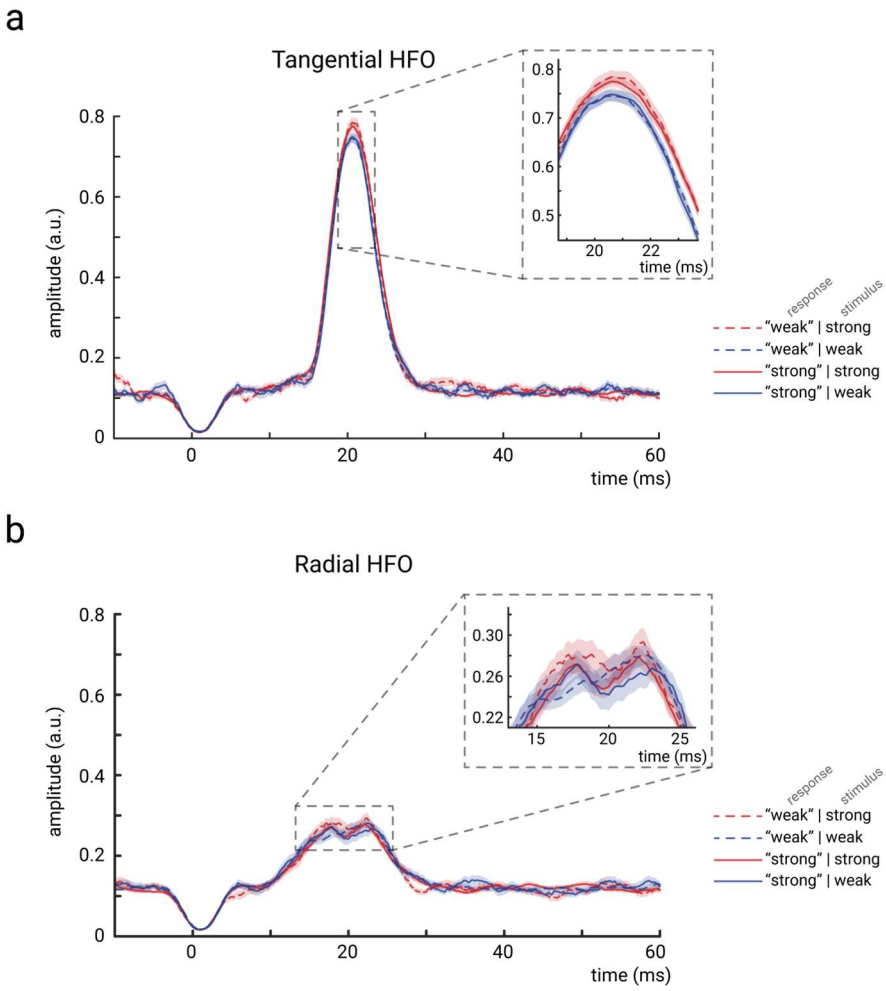

Fig. 4. Relationship between HFO and the perceived stimulus intensity.
a) No effect of HFO on the *perceived* stimulus intensity can be observed for the tangential CCA component when controlling for the *presented* stimulus intensity.
b) Similarly, no effect of HFO on perceived stimulus intensity emerged for the radial CCA component. Please note that trial sub-sampling was performed both in panel a and b, in order to account for different noise levels (i.e., baseline activity) that resulted from smaller trial numbers in the conditions *"weak"|strong* and *"strong"|weak* as compared to *"weak"|weak* and *"strong"|strong*. All curves reflect group-level averages of HFO envelopes; shaded areas correspond to the standard error of the mean based on the within-subject variances (Morey, 2008).

HFO are not affected by pre-stimulus alpha amplitude and only weakly related to N20 peaks

Since previous work found relationships between pre-stimulus alpha band amplitude and stimulus-evoked activity in conventional frequency bands, we tested for such a relationship also in HFO activity. The same pre-stimulus alpha activity that affected N20 amplitudes in our previous study (Stephani et al., 2021) did not show any effect on HFO amplitude, as tested with a linear-mixed effects model, β = -.007, t(24106.4) = -0.957, p = .338. Furthermore, Bayesian statistics provided moderate to strong evidence for the absence of an effect, BF01 = 8.65, β_{Bayes} = -.007, 95%-credibility interval = [-.021, .007]. (Very similar statistical results were obtained from the LMEs when not using the pre-stimulus alpha metric from our previous study but instead pre-stimulus alpha activity derived from the CCA filters trained to detect HFO for the current study, β = -.007, t(20834.2) = -0.900, p = .368.)

HFO and N20 amplitudes did show a significant relationship, β = -.013, t(26352.7) = -2.457, p = .014 (frequentist LME analysis), yet corresponding to only weak evidence for H1 according to the Bayesian approach, BF10 = 1.14, β_{Bayes} = -.013, 95%-credibility interval = [-.022, -.002]. The negative effect direction indicates that larger HFO amplitudes were associated with more negative N20 peak

amplitudes (i.e. larger magnitudes) which is also the effect direction that should be expected based on the effects of presented stimulus intensity on both N20 and HFO (but please note that we included stimulus intensity as a covariate in this analysis; thus, the weak yet significant relationship between N20 and HFO remains beyond trivial effects of stimulus intensity changes).

In summary, HFO amplitudes did thus not covary at all with the previously identified marker of excitability fluctuations in alpha amplitude fluctuations and were only weakly associated with the N20 peak amplitude of the conventional event-related response, which emerges at the very same time but in a lower frequency band.

Comparison of pre- versus post-N20 HFO

In order to exclude the possibility that our analyses of tangential HFO did not only reflect intra-cortical processes of somatosensory pyramidal cells but also pre-synaptic signals originating from thalamocortical axon terminals with a similar spatial orientation (Gobbelé et al., 2004), we additionally examined HFO occurring in the 3 ms *after* the N20 peak only. Results of the Bayesian linear-mixed-effects models for the relationships between HFO and perceived stimulus intensity, HFO and N20, as well as HFO and pre-stimulus alpha amplitude yielded very similar results as in above analyses for the whole time window, $BF01_{perceived} = 6.28$, $\beta_{perceived} = .008$, 95%-credibility $interval_{perceived} = [-.019, .035]$, $BF01_{N20} = 2.61$, $\beta_{N20} = -.011$, 95%-credibility $interval_{N20} = [-.021, .000]$, as well as $BF01_{prestim} = 7.75$, $\beta_{prestim} = -.008$, 95%-credibility $interval_{prestim} = [-.022, .006]$. When testing pre-N20 HFO (in a time window starting 3 ms before the N20 peak), no other effects emerged either, with Bayes factors being similar or even higher in favor of the null hypotheses, $BF01_{perceived} = 5.26$, $BF01_{N20} = 5.95$, $BF01_{prestim} = 10.6$. Thus, it is unlikely that the lack of relation between HFO and our other measures of interest was due to a mixed nature of pre- and post-synaptic HFO. Furthermore, this post-hoc analysis suggests that our findings are valid even when isolating the late part of HFO that can only be of intra-cortical origin, that is, presumably free from any thalamic contribution.

Discussion

Re-examining an EEG dataset of a somatosensory intensity discrimination paradigm (Stephani et al., 2021), we here tested the involvement of neuronal population spikes in moment-to-moment dynamics of neural excitability and their effects on perceived stimulus intensity. For this, we analyzed so-called high-frequency oscillations (HFO), stimulus-evoked oscillation-like responses in a frequency range around 700 Hz, which have previously been shown to reflect population spiking activity of the initial thalamocortical feedforward sweep of the somatosensory response cascade (Baker et al., 2003; Curio, 2000). Using Bayesian statistics, we found evidence against the involvement of HFO in behaviorally relevant excitability dynamics. Thus, population spiking activity of the first feedforward excitatory input does not seem to be involved in state-dependent modulation of sensory processes. Instead, following the notion that conventional evoked potentials in lower frequencies – such as the N20 component (Stephani et al., 2021) – may reflect a backpropagation of membrane potentials towards the apical dendrites, we suggest that top-down modulatory processes (e.g., related to alpha oscillations) take place at distal sites of the involved pyramidal cells rather than at basal compartments.

Evidence against the involvement of population spiking activity in the modulation of perceived stimulus intensity

The principal aim of the current study was to test whether high-frequency oscillations (HFO), interpreted as a measure of population spiking activity (Baker et al., 2003; Curio, 2000; Waterstraat et al., 2021; Hu et al., 2023; Shimazu et al., 2000; Ozaki & Hashimoto, 2011), respond to the physical intensity of the presented stimulus as well as encode fluctuations of the subjectively perceived stimulus

intensity. Previous studies, based on local field potentials, extracellular single unit recordings and surface EEG in non-human animals concluded that it is very likely that the intracortical component of HFO originate from the same pyramidal cells as the N20 potential (Shimazu et al., 2000; Ikeda et al., 2005; Baker et al., 2003). Furthermore, HFO are not an artifact of electrical nerve stimulation but are present in naturalistic tactile stimulation as well (Baker et al., 2003).

In line with previous work on HFO in humans (Klostermann et al., 1998; Gobbelé et al., 2008), we observed that a higher presented stimulus intensity led to larger HFO amplitudes. It is noteworthy that – in contrast to previous studies – the presented stimulus intensities here differed only very slightly regarding their somatosensory percept since we deliberately adjusted them to be close to the *just-noticeable difference*. Thus, even minute differences in the presented stimulus intensity appear to be encoded in HFO amplitudes. This makes sense in the context of HFO reflecting feedforward population spiking activity, that is, the forward propagation (i.e., output) of sensory processing at initial cortical levels. However, despite this robust relationship between HFO and presented stimulus intensity, we did not observe any association of HFO with the variability of the actually perceived stimulus intensity (i.e., when controlling for the presented stimulus intensity). In other words, trial-to-trial fluctuations of HFO did not make a difference for the participants´ ratings of the stimuli to feel stronger or weaker. This observation was supported by generalized linear-mixed effects modeling on a single-trial level, information theoretical comparisons of competing models, and cluster-based permutation statistics performed on participant-level average responses. In fact, additional Bayesian statistics even provided moderate evidence *against* the involvement of HFO in the modulation of perceived stimulus intensity. Moreover, we also tested this for post-N20 HFO separately, thus making sure that our findings cannot be biased by pre-synaptic HFO from thalamocortical axon terminals (Gobbelé et al., 2004; Ritter et al., 2008), thus further supporting the intra-cortical origin of our findings.

Taken together, we conclude that changes of feedforward population spiking activity merely reflect the sensory input but not any modulation exerted by early cortical integration processes or caused by spontaneous fluctuations of cortical excitability – in contrast to canonical SEP responses, such as the N20 component (Stephani et al., 2021), which are generally believed to reflect post-synaptic potentials instead of spiking activity (Kandel et al., 2000; Ilmoniemi & Sarvas, 2019; Lopes da Silva, 2004).

Importantly, the evidence *against* the involvement of first cortical feedforward spikes in the modulation of sensory processing (both behaviorally and neurally) in turn also suggests that modulation of sensory input did not occur at a first-order thalamic processing stage prior to the processing in S1. This thus lends further support to the notion that the spontaneous excitability fluctuations we observed in the present recording indeed reflect a cortical phenomenon.

Cortical task-related HFO in humans reside at frequencies around 700 Hz

Conventionally, HFO in the somatosensory domain of humans are assumed to arise in a frequency band around 600 Hz, so-called σ bursts (Curio, 2000; Waterstraat et al., 2016). Yet, our data rather suggested slightly higher frequencies, centered at 700 Hz (Fig. 2b). We were surprised by this observation and reviewed the literature on study designs similar to ours (i.e., median nerve stimulation with similar frequency and intensity). In fact, it appears from spectral and time frequency analyses reported in previous studies which also focused on tangentially oriented σ bursts, that HFO peak frequencies were clearly higher than 600 Hz and rather approaching 700 Hz (e.g., Waterstraat et al., 2021; Waterstraat et al., 2016; Hashimoto et al., 1996). Also when studying a presumably mixed signal of both tangential and radial HFO, peak frequencies exceeded 600 Hz (Ritter et al., 2008). In the latter study, an increase of HFO frequency was moreover associated with a decrease in stimulation frequency (tested for stimulation frequencies of 15Hz, 8Hz, and 4Hz). It is thus conceivable that the length of inter-stimulus intervals plays an important role for HFO frequency, as has also been observed by Klostermann et al. (1999). Given that our stimulation frequency was fairly low (on average 0.66 Hz), which should

avoid strong trial-to-trial attenuation effects, we thus assume that in situations where somatosensory stimuli are perceived in isolation (and not in the form of a pulse train as in passive stimulation paradigms), cortical HFO may in fact reside in a higher frequency range than the conventionally reported 600 Hz. In addition, the distinction between even higher frequency ranges is important in this context. Besides the σ bursts (conventionally 600 Hz; in our study 700 Hz), two other HFO classes of even higher frequencies have been documented: kappa1 (800-1150 Hz) and kappa2 (1100-2000 Hz; Fedele et al., 2012; Scheer et al., 2011). Although a partial overlap of σ and kappa1 activity cannot be excluded for the HFO components in our study, we suggest interpreting our HFO activity in the context of σ bursts, which has been shown to consist of radial and tangential sub-components (Gobbelé et al., 2004; Fedele et al., 2012; Ozaki et al., 1998; Ozaki & Hashimoto, 2011; Waterstraat et al., 2016) – exactly corresponding to what we observed with our CCA decomposition (Fig. 2c & d).

Given that our study was among the first attempts to probe the behavioral relevance of HFO variability (i.e., the effect of HFO amplitude on perceived stimulus intensity), the here observed frequency shift towards 700 Hz may thus be important to consider in future studies that examine HFO in psychophysics paradigms.

Excitability-related modulation of sensory input may emerge through backpropagating membrane potentials

Employing Bayesian statistics, the current study provides evidence *against* the involvement of neuronal population spiking activity (HFO) in the variability of neuronal processing at initial cortical stages regarding the perceived stimulus intensity. In other words, not the signals that are sent down-stream from S1 pyramidal cells (i.e., action potentials/ spiking activity) seem to be modulated by spontaneous neuronal states (such as excitability) but instead the post-synaptic membrane potentials that stay within the pyramidal cells (i.e., the N20 potential) and that propagate "back" in soma-dendritic direction. Here we also assume that both HFO and N20 are generated largely by the same neurons (see above). Thus, our data are in line with the interpretation of neural states shaping pyramidal cell depolarization along the apical dendrites but not regarding their output firing activity at basal pyramidal cell compartments – at least not during the initial cortical feedforward volley. This may also explain why the relation between alpha band oscillations and neuronal firing activity are typically found to be rather small, even in animal work with invasive recordings (e.g., Haegens et al., 2011).

Although it may seem puzzling that low-frequency SEP activity, which reflects post-synaptic membrane potentials (Lopes da Silva, 2004; Ilmoniemi & Sarvas, 2019; Næss et al., 2021), does not directly translate into the neuron´s firing output, our observations of partly independent N20 and HFO dynamics complement the previous literature very well. For instance, it has been reported that the N20 shows small increments when entering deep sleep stages while HFO are drastically diminished (Hashimoto et al., 1996). Furthermore, the N20 and HFO are affected differentially by propofol anesthesia: Whereas the N20 remains stable, HFO are substantially decreased both in amplitude and frequency (Klostermann et al., 2000). Additionally, HFO were found to be increased in eyes-open as compared to eyes-closed EEG recordings while the N20 appears to be unaffected (Gobbelé et al., 2008). In contrast, isometric motor contraction leads to an attenuation of the N20 but not of HFO (Klostermann et al., 2001). Such motor gating of the somatosensory domain has been proposed to emerge via efference copies (Holst, 1954; Wolpert & Ghahramani, 2000; Palmer et al., 2016; Kilteni et al., 2020; Job & Kilteni, 2023) and may act via layer 1 top-down projections (Manita et al., 2015; Manita et al., 2017), thus potentially reflecting a mechanism in line with Dendritic Integration Theory. Last but not least, transcranial alternating current stimulation (tACS) at alpha frequencies has been reported to up-regulate N20 amplitudes but not HFO (Fabbrini et al., 2022). Together, these studies provide compelling evidence of the differential functional properties of the N20 component and HFO.

Nevertheless, our data showed a weak but significant covariation of N20 and HFO amplitudes – in contrast to a previous study (Waterstraat et al., 2021) – even when controlling for the presented stimulus intensity. The simplest explanation for that may be our considerably higher sample size (N=27 vs. N=4) and thus higher statistical power. It should indeed be expected that N20 and HFO are somewhat related given that the N20 and at least the late portion of the tangentially oriented HFO are believed to originate from the same pyramidal cells in S1 that are involved in the initial sensory feedforward volley (Ikeda et al., 2005; Baker et al., 2003). However, it is also conceivable that spontaneous changes of signal-to-noise ratio had a common influence on both N20 and HFO amplitudes (although we detrended all neural measures to account for slow trends over the course of the experiment). Thus, there may be some partial, yet not conclusive overlap of variance between N20 and HFO fluctuations, which however does not seem to be of behavioral relevance in sensory processing when tested with the approaches used in our study.

Following the notion that HFO are generated at basal regions of cortical pyramidal cells (Baker et al., 2003; Curio, 2000; Shimazu et al., 2000; Hu et al., 2023) while the N20 component reflects post-synaptic membrane potentials that propagate back along the apical dendrites towards superficial layers (Wikström et al., 1996; Bruyns-Haylett et al., 2017; Thorpe et al., 2024), the lack of behaviorally relevant HFO fluctuations in the current study in combination with the effects of N20 and alpha band amplitudes in our previous study (Stephani et al., 2021) suggests that moment-to-moment changes of the perceived stimulus intensity are mediated by top-down modulations in apical rather than basal dendritic compartments. This is not only well in line with Dendritic Integration Theory (Bachmann et al., 2020; Aru et al., 2020; Larkum, 2022) but also complies with recent observations of alpha band activity exerting a top-down influence on superficial layers of primary sensory regions (Halgren et al., 2019), as well as with earlier conceptions of the interplay between re-entrant bottom-up and top-down signals in superficial layers at early stages of the somatosensory response cascade (Cauller, 1995; Cauller & Kulics, 1991). In this context, it is noteworthy that also HFO result in membrane potentials that travel in soma-dendritic direction (Ikeda et al., 2005), yet at the frequency of HFO and thus possibly resembling back-propagating action potentials (Buzsáki & Kandel, 1998; Waters et al., 2005). According to the measurement principles of M/EEG, it is conceivable that our HFO signals reflected these additional manifestations of the neuronal output firing rather than the axonal action potentials themselves. Nevertheless, this is still in line with our interpretation since the back-propagating action potentials are expected to be proportional to their outgoing counterparts.

Moreover, it remains an open question what happens to the backpropagating post-synaptic potentials that are visible in the EEG as the N20 component. Which subsequent neuronal processes use this information and in what way does this affect sensory information processing down-stream? A tentative hypothesis may be that the backpropagated N20 potential serves the function of a "neuronal buffer", that is, a trace of the immediate past of sensory exposure within specific pyramidal cells/ pyramidal cell populations. In line with previously observed trial-to-trial temporal dependencies for perceptual decision making in general (Urai et al., 2019; Forster et al., 2024) and for early somatosensory potentials in particular (Stephani et al., 2020; Stephani et al., 2022), this information may then be integrated with both top-down as well as subsequent bottom-up sensory input. Yet, to test this, approaches are required that are able to deliberately modulate apical dendritic activity which was not possible with the current study design.

Conclusions

In the current work, we found evidence *against* the involvement of feedforward neuronal population spikes (non-invasively assessed by high-frequency oscillations, HFO) in moment-to-moment variability of the perceived intensity of somatosensory stimuli. Given that behaviorally relevant modulations of both pre-stimulus alpha activity and N20 amplitudes of the SEP were found in previous

analyses of the same dataset, we suggest that these discrepancies can be explained by top-down excitability changes that act on *apical* rather than *basal* dendritic compartments. Thus, not the output of the first feedforward sweep seems to be affected by instantaneous neural states in somatosensory processing but rather its backpropagating counterpart in form of post-synaptic potentials in soma-dendritic direction.

Materials and Methods

This research advance builds on the dataset and part of the analyses of Stephani et al., 2021, published in *eLife*. For detailed information regarding the participants, stimuli, experimental procedure, and data acquisition, please refer to the respective sections in the corresponding original research article [link to *Materials and methods*: https://elifesciences.org/articles/67838#s4].

Particularly, EEG pre-processing and signal extraction of the N20 response of the somatosensory evoked potential (SEP), as well as of pre-stimulus alpha band activity, were identical as in our previous study. In the following, we report the specific pre-processing steps that we used to extract high-frequency oscillations (HFO) as well as subsequently employed statistical procedures.

Pre-processing and signal extraction of HFO

General EEG pre-processing for the extraction of high-frequency oscillations (HFO) was similar as in our previous analysis (Stephani et al., 2021) yet deviating regarding the EEG frequency range of interest: The EEG data were band-pass filtered between 550 and 850 Hz with a sixth-order Butterworth filter (applied forwards and backwards to prevent phase shift). This filter was tuned to HFO activity centered around 700 Hz with a range of ±150 Hz (as was indicated to be appropriate by prior time-frequency analyses). The same data segments and the same ICA components were removed as in the previous analyses, leading to the same amount of trials of HFO activity as in our original work.

Again, we used canonical correlation analysis (CCA) to find spatial filters that optimized the signal-to-noise ratio of single-trial evoked activity – a method that was developed for HFO specifically (Fedele et al., 2013; Waterstraat et al., 2015). Deviating from our previous analysis of conventional SEP (i.e., N20 component), we here trained the CCA weights in time windows from 10 to 30 ms (but, again, applied the resulting spatial filters to the whole data epochs from -100 to 600 ms). The resulting CCA components were visually inspected regarding their stimulus-locked time courses and spatial activation patterns. This was done for each participant individually. CCA components that showed HFO activity around 20 ms post-stimulus *and* a spatial activation pattern indicating a tangentially oriented dipole were selected for further analysis (referred to as *tangential CCA component*; Fig. 2C). In contrast, CCA components that showed a unipolar activation pattern over the right primary somatosensory cortex were classified as *radial CCA components*. The tangential CCA components were always found to be the CCA components with the highest canonical correlation coefficients, while the radial CCA components were always second. For a more detailed description of the CCA decomposition approach, please refer to our original article (Stephani et al., 2021). Using this approach to obtain spatial filters that optimized for stimulus-locked high-frequency activity, HFO were possible to observe in 27 out of 32 participants (indicated by visual inspection of spatial activation patterns and single-trial, as well as average evoked responses). In order to extract the amplitude of HFO on a single-trial basis, we quantified the area-under-the-curve (AUC) of the Hilbert envelope, measured in a time interval of ±3 ms around the latency of the N20 component (individually determined based on the within-participant average SEP). In an additional analysis, we split that time window and extracted the AUC of the HFO envelope both in the window 3 ms before and after the individually determined N20 peak separately (referred to as pre- and post-N20 HFO).

Time-frequency representations of HFO were computed using complex Morlet wavelets between 40 and 1250 Hz, with cycle numbers logarithmically scaled from 3 to 20 (60 frequencies in total).

For the visualization and cluster-based permutation tests of the average HFO envelopes of different behavioral response categories, additional sub-sampling of the trials was required since response categories differed in their numbers (arithmetic means of trial numbers per response category: $N_{\text{"strong"}|\text{strong}}$=341.9; $N_{\text{"weak"}|\text{strong}}$=145.6; $N_{\text{"strong"}|\text{weak}}$=140.0; $N_{\text{"weak"}|\text{weak}}$=349.4). As could be expected, higher trial numbers resulted in a lower noise level (and thus lower baseline activity) of the averaged HFO envelopes than lower trial numbers. Trial sub-sampling was performed as follows (individually performed for each participant): The amount of trials in the response condition with the least trials was randomly selected from the other response conditions and averaged. This procedure was repeated 1000 times and the resulting sub-averages were in turn averaged, in order to account for the random selection of trials that went into the sub-averages and to obtain stable estimates of the HFO envelopes in response conditions with different trial numbers. Single-trial statistics were performed without sub-sampling since the factors *presented stimulus intensity* and *perceived stimulus intensity* were explicitly modelled here and the effects of unequal trial numbers should cancel each other out, given the fully crossed experimental design.

Statistics

Generalized linear mixed-effects models were employed to examine the relationships between *HFO amplitude*, *presented stimulus intensity*, *N20 amplitude*, *pre-stimulus alpha amplitude*, as well as *perceived stimulus intensity* on a single-trial level. For reasons of model convergence and comparability across models, random-intercept models were computed in all cases (with random factor *subject*). We tested the following models:

(1) *HFO* ~ 1 + *presented stimulus intensity* + (1 | *subject*) ,

(2) *Perceived stimulus intensity* ~ 1+ *presented stimulus intensity* + *prestimulus alpha* + *N20* + *HFO* + (1 | *subject*) ,

(3) *Perceived stimulus intensity* ~ 1+ *presented stimulus intensity* + *HFO* + (1 | *subject*) ,

(4) *HFO* ~ 1 + *presented stimulus intensity* + *prestimulus alpha* + (1 | *subject*) ,

(5) *N20* ~ 1 + *presented stimulus intensity* + *HFO* + (1 | *subject*) .

A logit link function was used in case of *perceived stimulus intensity* being the dependent variable, in order to account for its dichotomous scale. Before any statistics, pre-stimulus alpha amplitudes were log-transformed in order to approximate a normal distribution, and all continuous variables were z-transformed. Furthermore, to ensure that no longitudinal trends over the course of the experiment drove the effects of interest (time-on-task effect; Benwell et al., 2019), we detrended *prestimulus alpha amplitudes*, *N20 amplitudes*, and *HFO amplitudes* across trials by regressing out the predictor *trial_index* before subjecting these measures to the generalized linear-mixed effects models described above.

Model comparisons were evaluated using the likelihood ratio test (LRT), the Akaike Information Criterion (AIC), and the Bayesian Information Criterion (BIC). The significance level for all analyses was set to p = .05 (two-sided).

Complementarily, Bayesian statistics were based on the regression models (3), (4), and (5) described above, and computed with 4 Markov chain Monte Carlo (MCMC) chains of 6000 iterations each. Priors for the fixed effects of interest were chosen to be normally distributed around a mean of 0

with a standard deviation of 0.1 based on the scaling of effects in Stephani et al., 2021 (i.e., corresponding to a weakly informative prior; McElreath, 2020).

Cluster-based permutation tests were performed for additional testing of the relationships between *HFO amplitude* and *presented stimulus intensity* as well as *perceived stimulus intensity*. For the latter, separate analyses were conducted for strong and weak presented stimuli. In all cases, 10000 permutations of the condition labels of interest were conducted, group-level paired-sample *t*-tests were used to compare the resulting condition differences, and clusters were formed with a pre-threshold of $p_{pre} = .05$, thus resulting in the null distribution for the hypothesis test (sum of *t* values in each cluster). The empirical *t*-value sum was subsequently compared with this null distribution and deemed significant if being more extreme than 5% of the values of the null distribution, corresponding to a cluster significance level of $p_{cluster} = .05$. In addition, we performed the same cluster analysis a second time but with $p_{cluster} = .1$ for the relationship between HFO and perceived stimulus intensity, in order to decrease the type II error of not detecting a true difference (in the context of our interpretation of the null effect here). In order to account for different trial numbers of correct and incorrect behavioral responses, we performed a trial sub-sampling approach for the cluster-based permutation tests regarding the effects on perceived stimulus intensity. This was required since we here split the analysis into strong and weak presented stimulus intensities, which resulted in unbalanced trial numbers for weak stimuli being rated as weak stimuli as compared to weak stimuli being rated as strong stimuli (and correspondingly for the strong presented stimuli; note that the task accuracy rate was around 70% in both conditions – thus markedly above chance level – leading to reduced trial numbers of the incorrect responses [conditions *"weak"|strong* and *"strong"|weak*]). We performed the trial sub-sampling for every participant separately in the following way: First, we drew as many trials from all four behavioral conditions (presented intensity x perceived intensity) as the condition with the fewest trials contained. These trials were randomly drawn (with replacement) and the procedure was repeated 1000 times. Subsequently, we averaged the HFO signals within each of these sub-samples and computed their Hilbert envelopes. The arithmetic mean of these 1000 sub-sampling envelopes then served as our participant-level average HFO envelope, which was subjected to the cluster-based permutation statistics. Also, we use these trial-number controlled HFO envelopes for visualization in Figure 4.

The permutation-based analyses were performed in MATLAB (version 2022b, The MathWorks Inc, Natick, MA). The generalized linear mixed-effects models were calculated in R (version 4.2.2, R Development Core Team, 2018). For the frequentist approach, the lme4 package (version 1.1–30, Bates et al., 2015) was used, estimating the fixed-effect coefficients based on the restricted maximum likelihood (REML). To derive a p value for the fixed-effect coefficients, the denominator degrees of freedom were adjusted using Satterthwaite's method (Satterthwaite, 1946) as implemented in the R package lmerTest (version 3.1–3, Kuznetsova et al., 2017). The Bayesian analyses were performed with the brms package (version 2.17.0, Bürkner, 2017).

Open code and open data statements

The code for data analysis as well as the data used for summary statistics and for generating the figures are accessible at: https://osf.io/meyza/?view_only=c43d4bc78bac4b72b1674af19c5ddf89. The raw EEG data cannot be made available in a public repository due to the privacy policies for human biometric data according to the European General Data Protection Regulation (GDPR). Further preprocessed data can be obtained from the corresponding author (TS; tilman.stephani@donders.ru.nl) upon reasonable request and as far as the applicable data privacy regulations allow it.

Acknowledgements

We very much thank Gabriel Curio and Gunnar Waterstraat for discussions of the HFO results presented in this manuscript.

References

Allison, T., McCarthy, G., Wood, C. C., & Jones, S. J. (1991). Potentials Evoked in Human and Monkey Cerebral Cortex by Stimulation of the Median Nerve. *Brain*, *114*, 2465–2503.

Arieli, A., Sterkin, A., Grinvald, A., & Aertsen, A. (1996). Dynamics of ongoing activity: Explanation of the large variability in evoked cortical responses. *Science*, *273*, 1868–1871.

Aru, J., Suzuki, M., & Larkum, M. E. (2020). Cellular Mechanisms of Conscious Processing. *Trends in Cognitive Sciences*, *24*, 814–825.

Bachmann, T., Suzuki, M., & Aru, J. (2020). Dendritic integration theory: A thalamo-cortical theory of state and content of consciousness. *Philosophy and the Mind Sciences*, *1*, 2.

Baker, S. N., Curio, G., & Lemon, R. N. (2003). EEG oscillations at 600 Hz are macroscopic markers for cortical spike bursts. *The Journal of physiology*, *550*, 529–534.

Bates, D., Mächler, M., Bolker, B., & Walker, S. (2015). Fitting Linear Mixed-Effects Models Using lme4. *Journal of Statistical Software*, *67*, 1–48.

Benwell, C. S., London, R. E., Tagliabue, C. F., Veniero, D., Gross, J., Keitel, C., & Thut, G. (2019). Frequency and power of human alpha oscillations drift systematically with time-on-task. *NeuroImage*, *192*, 101–114.

Bruyns-Haylett, M., Luo, J., Kennerley, A. J., Harris, S., Boorman, L., Milne, E., Vautrelle, N., Hayashi, Y., Whalley, B. J., Jones, M., Berwick, J., Riera, J., & Zheng, Y. (2017). The neurogenesis of P1 and N1: A concurrent EEG/LFP study. *NeuroImage*, *146*, 575–588.

Bürkner, P.-C. (2017). brms An R Package for Bayesian Multilevel Models Using Stan. *Journal of Statistical Software*, *80*, 1–28.

Buzsáki, G., & Kandel, A. (1998). Somadendritic backpropagation of action potentials in cortical pyramidal cells of the awake rat. *Journal of neurophysiology*, *79*, 1587–1591.

Cauller, L. (1995). Layer I of primary sensory neocortex: where top-down converges upon bottom-up. *Behavioural brain research*, *71*, 163–170.

Cauller, L. J., & Kulics, A. T. (1991). The neural basis of the behaviorally relevant N1 component of the somatosensory-evoked potential in SI cortex of awake monkeys: evidence that backward cortical projections signal conscious touch sensation. *Experimental brain research*, *84*, 607–619.

Curio, G. (2000). Linking 600-Hz "spikelike" EEG/MEG wavelets ("sigma-bursts") to cellular substrates: concepts and caveats. *Journal of Clinical Neurophysiology*, *17*, 377–396.

Fabbrini, A., Guerra, A., Giangrosso, M., Manzo, N., Leodori, G., Pasqualetti, P., Conte, A., Di Lazzaro, V., & Berardelli, A. (2022). Transcranial alternating current stimulation modulates cortical processing of somatosensory information in a frequency- and time-specific manner. *NeuroImage*, *254*, 119119.

Fedele, T., Scheer, H. J., Waterstraat, G., Telenczuk, B., Burghoff, M., & Curio, G. (2012). Towards non-invasive multi-unit spike recordings: mapping 1kHz EEG signals over human somatosensory cortex. *Clinical neurophysiology official journal of the International Federation of Clinical Neurophysiology*, *123*, 2370–2376.

Fedele, T., Scheer, H.-J., Burghoff, M., Waterstraat, G., Nikulin, V. V., & Curio, G. (2013). Distinction between added-energy and phase-resetting mechanisms in non-invasively detected somatosensory evoked responses. *Conference proceedings: IEEE Engineering in Medicine and Biology Society. Annual Conference*, *2013*, 1688–1691.

Forster, C., Stephani, T., Grund, M., Panagoulas, E., Al, E., Hofmann, S. M., Nikulin, V. V., & Villringer, A. (2024). Pre-stimulus beta power encodes explicit and implicit perceptual biases in distinct cortical areas. *bioRxiv*.

Gobbelé, R., Dieckhöfer, A., Thyerlei, D., Buchner, H., & Waberski, T. D. (2008). The impact of stimulus properties on low- and high-frequency median nerve somatosensory evoked potentials. *Journal of clinical neurophysiology official publication of the American Electroencephalographic Society*, *25*, 194–201.

Gobbelé, R., Waberski, T. D., Kuelkens, S., Sturm, W., Curio, G., & Buchner, H. (2000). Thalamic and cortical high-frequency (600 Hz) somatosensory-evoked potential (SEP) components are modulated by slight arousal changes in awake subjects. *Experimental brain research*, *133*, 506–513.

Gobbelé, R., Waberski, T. D., Simon, H., Peters, E., Klostermann, F., Curio, G., & Buchner, H. (2004). Different origins of low- and high-frequency components (600 Hz) of human somatosensory evoked potentials. *Clinical Neurophysiology*, *115*, 927–937.

Haegens, S., Nácher, V., Luna, R., Romo, R., & Jensen, O. (2011). α-Oscillations in the monkey sensorimotor network influence discrimination performance by rhythmical inhibition of neuronal spiking. *Proceedings of the National Academy of Sciences*, *108*, 19377–19382.

Halgren, M., Ulbert, I., Bastuji, H., Fabó, D., Erőss, L., Rey, M., Devinsky, O., Doyle, W. K., Mak-McCully, R., Halgren, E., Wittner, L., Chauvel, P., Heit, G., Eskandar, E., Mandell, A., & Cash, S. S. (2019). The generation and propagation of the human alpha rhythm. *Proceedings of the National Academy of Sciences*, *116*, 23772–23782.

Hashimoto, I., Mashiko, T., & Imada, T. (1996). Somatic evoked high-frequency magnetic oscillations reflect activity of inhibitory interneurons in the human somatosensory cortex. *Electroencephalography and Clinical Neurophysiology/Evoked Potentials Section*, *100*, 189–203.

Holst, E. von (1954). Relations between the central Nervous System and the peripheral organs. *The British Journal of Animal Behaviour*, *2*, 89–94.

Hu, H., Hostetler, R. E., & Agmon, A. (2023). Ultrafast (400 Hz) network oscillations induced in mouse barrel cortex by optogenetic activation of thalamocortical axons. *eLife*, *12*, e82412.

Ikeda, H., Wang, Y., & Okada, Y. C. (2005). Origins of the somatic N20 and high-frequency oscillations evoked by trigeminal stimulation in the piglets. *Clinical neurophysiology official journal of the International Federation of Clinical Neurophysiology*, *116*, 827–841.

Ilmoniemi, R., & Sarvas, J. (2019). *Brain signals: Physics and mathematics of MEG and EEG*. Cambridge: The MIT Press.

Job, X., & Kilteni, K. (2023). *Action does not enhance but attenuates predicted touch*.

Kandel, E. R., Schwartz, J. H., & Jessell, T. M. (Eds.) (2000). *Principles of neural science.* (4. ed.). New York, NY: McGraw-Hill Health Professions Division.

Kilteni, K., Engeler, P., & Ehrsson, H. H. (2020). Efference Copy Is Necessary for the Attenuation of Self-Generated Touch. *iScience*, *23*, 100843.

Klostermann, F., Funk, T., Vesper, J., Siedenberg, R., & Curio, G. (2000). Propofol narcosis dissociates human intrathalamic and cortical high-frequency (400 hz) SEP components. *Neuroreport*, *11*, 2607–2610.

Klostermann, F., Gobbele, R., Buchner, H., Siedenberg, R., & Curio, G. (2001). Differential gating of slow postsynaptic and high-frequency spike-like components in human somatosensory evoked potentials under isometric motor interference. *Brain Research*, *922*, 95–103.

Klostermann, F., Nolte, G., & Curio, G. (1999). Multiple generators of 600 Hz wavelets in human SEP unmasked by varying stimulus rates. *Neuroreport*, *10*, 1625–1629.

Klostermann, F., Nolte, G., Losch, F., & Curio, G. (1998). Differential recruitment of high frequency wavelets (600 Hz) and primary cortical response (N20) in human median nerve somatosensory evoked potentials. *Neuroscience letters*, *256*, 101–104.

Kulics, A. T., & Cauller, L. J. (1986). Cerebral cortical somatosensory evoked responses, multiple unit activity and current source-densities: their interrelationships and significance to somatic sensation as revealed by stimulation of the awake monkey's hand. *Experimental brain research*, *62*, 46–60.

Kuznetsova, A., Brockhoff, P. B., & Christensen, R. H. B. (2017). lmerTest Package: Tests in Linear Mixed Effects Models. *Journal of Statistical Software*, *82*, 1–26.

Larkum, M. (2013). A cellular mechanism for cortical associations: an organizing principle for the cerebral cortex. *Trends in Neurosciences*, *36*, 141–151.

Larkum, M. (2022). Are dendrites Conceptually Useful? *Neuroscience*, *489*, 4-14.

Larkum, M. E., Kaiser, K. M., & Sakmann, B. (1999). Calcium electrogenesis in distal apical dendrites of layer 5 pyramidal cells at a critical frequency of back-propagating action potentials. *Proceedings of the National Academy of Sciences*, *96*, 14600–14604.

Larkum, M. E., Senn, W., & Lüscher, H.-R. (2004). Top-down dendritic input increases the gain of layer 5 pyramidal neurons. *Cerebral Cortex*, *14*, 1059–1070.

Lopes da Silva, F. (2004). Functional localization of brain sources using EEG and/or MEG data: volume conductor and source models. *Magnetic resonance imaging*, *22*, 1533–1538.

Manita, S., Miyakawa, H., Kitamura, K., & Murayama, M. (2017). Dendritic Spikes in Sensory Perception. *Frontiers in cellular neuroscience*, *11*, 29.

Manita, S., Suzuki, T., Homma, C., Matsumoto, T., Odagawa, M., Yamada, K., Ota, K., Matsubara, C., Inutsuka, A., Sato, M., Ohkura, M., Yamanaka, A., Yanagawa, Y., Nakai, J., Hayashi, Y., Larkum, M. E., & Murayama, M. (2015). A Top-Down Cortical Circuit for Accurate Sensory Perception. *Neuron*, *86*, 1304–1316.

Marvan, T., Polák, M., Bachmann, T., & Phillips, W. A. (2021). Apical amplification—a cellular mechanism of conscious perception? *Neuroscience of consciousness*, *2021*, niab036.

McCormick, D. A., Nestvogel, D. B., & He, B. J. (2020). Neuromodulation of Brain State and Behavior. *Annual review of neuroscience*, *43*, 391–415.

McElreath, R. (2020). *Statistical rethinking: A Bayesian course with examples in R and Stan.* (Second edition). Chapman & Hall/CRC texts in statistical science series. Boca Raton, London, New York: CRC Press.

Morey, R. D. (2008). Confidence Intervals from Normalized Data: A correction to Cousineau (2005). *Tutorial in Quantitative Methods for Psychology*, *4*, 61–64.

Næss, S., Halnes, G., Hagen, E., Hagler, D. J., Dale, A. M., Einevoll, G. T., & Ness, T. V. (2021). Biophysically detailed forward modeling of the neural origin of EEG and MEG signals. *NeuroImage*, *225*, 117467.

Nicholson Peterson, N., Schroeder, C. E., & Arezzo, J. C. (1995). Neural generators of early cortical somatosensory evoked potentials in the awake monkey. *Electroencephalography and Clinical Neurophysiology/Evoked Potentials Section*, *96*, 248–260.

Ozaki, I., & Hashimoto, I. (2011). Exploring the physiology and function of high-frequency oscillations (HFOs) from the somatosensory cortex. *Clinical neurophysiology official journal of the International Federation of Clinical Neurophysiology*, *122*, 1908–1923.

Ozaki, I., Suzuki, C., Yaegashi, Y., Baba, M., Matsunaga, M., & Hashimoto, I. (1998). High frequency oscillations in early cortical somatosensory evoked potentials. *Electroencephalography and clinical neurophysiology*, *108*, 536–542.

Palmer, C. E., Davare, M., & Kilner, J. M. (2016). Physiological and Perceptual Sensory Attenuation Have Different Underlying Neurophysiological Correlates. *The Journal of Neuroscience*, *36*, 10803–10812.

Phillips, W. A., Clark, A., & Silverstein, S. M. (2015). On the functions, mechanisms, and malfunctions of intracortical contextual modulation. *Neuroscience and biobehavioral reviews*, *52*, 1–20.

Phillips, W. A., Larkum, M. E., Harley, C. W., & Silverstein, S. M. (2016). The effects of arousal on apical amplification and conscious state. *Neuroscience of consciousness*, *2016*, niw015.

Ritter, P., Freyer, F., Curio, G., & Villringer, A. (2008). High-frequency (600 Hz) population spikes in human EEG delineate thalamic and cortical fMRI activation sites. *NeuroImage*, *42*, 483–490.

Sadaghiani, S., Hesselmann, G., Friston, K. J., & Kleinschmidt, A. (2010). The relation of ongoing brain activity, evoked neural responses, and cognition. *Frontiers in systems neuroscience*, *4*, 20.

Samaha, J., Iemi, L., Haegens, S., & Busch, N. A. (2020). Spontaneous Brain Oscillations and Perceptual Decision-Making. *Trends in Cognitive Sciences*, *24*, 639–653.

Satterthwaite, F. E. (1946). An Approximate Distribution of Estimates of Variance Components. *Biometrics Bulletin*, *2*, 110.

Scheer, H. J., Fedele, T., Curio, G., & Burghoff, M. (2011). Extension of non-invasive EEG into the kHz range for evoked thalamocortical activity by means of very low noise amplifiers. *Physiological measurement*, *32*, N73-9.

Shimazu, H., Kaji, R., Tsujimoto, T., Kohara, N., Ikeda, A., Kimura, J., & Shibasaki, H. (2000). High-frequency SEP components generated in the somatosensory cortex of the monkey. *Neuroreport*, *11*.

Stephani, T., Hodapp, A., Jamshidi Idaji, M., Villringer, A., & Nikulin, V. V. (2021). Neural excitability and sensory input determine intensity perception with opposing directions in initial cortical responses. *eLife*, *10*, e67838.

Stephani, T., Nierula, B., Villringer, A., Eippert, F., & Nikulin, V. V. (2022). Cortical response variability is driven by local excitability changes with somatotopic organization. *NeuroImage*, *264*, 119687.

Stephani, T., Waterstraat, G., Haufe, S., Curio, G., Villringer, A., & Nikulin, V. V. (2020). Temporal Signatures of Criticality in Human Cortical Excitability as Probed by Early Somatosensory Responses. *The Journal of Neuroscience*, *40*, 6572–6583.

Thorpe, R. V., Black, C. J., Borton, D. A., Hu, L., Saab, C. Y., & Jones, S. R. (2024). Distinct neocortical mechanisms underlie human SI responses to median nerve and laser-evoked peripheral activation. *Imaging Neuroscience*, *2*, 1–29.

Urai, A. E., Gee, J. W. de, Tsetsos, K., & Donner, T. H. (2019). Choice history biases subsequent evidence accumulation. *eLife*, *8*, e46331.

Waschke, L., Kloosterman, N. A., Obleser, J., & Garrett, D. D. (2021). Behavior needs neural variability. *Neuron*, *109*, 751–766.

Waters, J., Schaefer, A., & Sakmann, B. (2005). Backpropagating action potentials in neurones: measurement, mechanisms and potential functions. *Progress in biophysics and molecular biology*, *87*, 145–170.

Waterstraat, G., Fedele, T., Burghoff, M., Scheer, H.-J., & Curio, G. (2015). Recording human cortical population spikes non-invasively--An EEG tutorial. *Journal of neuroscience methods*, *250*, 74–84.

Waterstraat, G., Körber, R., Storm, J.-H., & Curio, G. (2021). Noninvasive neuromagnetic single-trial analysis of human neocortical population spikes. *Proceedings of the National Academy of Sciences*, *118*, e2017401118.

Waterstraat, G., Scheuermann, M., & Curio, G. (2016). Non-invasive single-trial detection of variable population spike responses in human somatosensory evoked potentials. *Clinical neurophysiology official journal of the International Federation of Clinical Neurophysiology*, *127*, 1872–1878.

Wikström, H., Huttunen, J., Korvenoja, A., Virtanen, J., Salonen, O., Aronen, H., & Ilmoniemi, R. J. (1996). Effects of interstimulus interval on somatosensory evoked magnetic fields (SEFs): A hypothesis concerning SEF generation at the primary sensorimotor cortex. *Electroencephalography and Clinical Neurophysiology/Evoked Potentials Section*, *100*, 479–487.

Wolpert, D. M., & Ghahramani, Z. (2000). Computational principles of movement neuroscience. *Nature Neuroscience*, *3 Suppl*, 1212–1217.